DEVELOPMENT OF NEW ADSORBENTS BASED ON ACTIVATED CARBON, MODIFIED ZEOLITES WITH HDTMA-Br AND GOETHITE FOR Cr(VI) REMOVAL

KARASAVVIDIS C.[1], IOANNOU Z.[2] and DIMIRKOU A.[1]

[1]Soil Science laboratory, Department of Agriculture, Crop Production & Rural Environment, University of Thessaly, Fytoko St., Volos, Magnesia, Greece, [2]Department of Food Science & Nutrition, University of the Aegean, 2 Metropolite Ioakeim St., Myrina, Limnos, Greece, tel. +30-22540-83122, fax. +30-22540-83109
E-mail: zioan@teemail.gr

ABSTRACT

In the present study, the removal of Cr(VI) from different adsorbents was studied. Raw materials such as goethite, zeolite, hexadecyltrimethylammonium-bromide (HDTMA-Br) and commercial activated carbon have been used for the production of goethite – modified zeolite (G-MZ I and II) and goethite-modified zeolite–activated carbon (G-MZ-C I and II). Modified zeolite and commercial activated carbon were added either at the beginning of goethite production or at the end. The produced materials were characterized through FTIR analysis. Aqueous solutions of Cr(VI) were prepared from $K_2Cr_2O_7$, in a concentration of 40 ppm. A batch operation was conducted with the proportion of adsorbent to adsorbate equal to 1/100 g/mL. Cr(VI) was determined with di-phenyl-carvazide method using VIS spectrophotometer at 540 nm. FTIR analysis has shown the presence of functional groups, i.e. Si-O, C-N, Al-O, –OH, -C-H, CH_3-R and Fe-O. According to the results, tripartite adsorbents (G–MZ –C II, G–MZ–C I) presented higher Cr(VI) adsorption compared to binary adsorbents (G–MZ I, G– MZ II). The adsorption capacity of adsorbents increases in the following order: G–MZ –C II $\geq$ G–MZ–C I> G– MZ I > G–MZ II. Moreover, a kinetic analysis was conducted using different models: pseudo first order, pseudo second order, Elovich kinetic equations and intraparticle diffusion model. From the application of the kinetic models, it is concluded that: (a) the intraparticle diffusion model is valid for the B and C region where macropore and mesopore diffusion takes place, respectively and (b) the Elovich kinetic model for the adsorption of Cr(VI) on all adsorbents for the C region. Such adsorbents are ideal for heavy metal removal from wastewaters.

Keywords: goethite, HDTMA-Br, zeolite, activated carbon, Cr(VI)

1. Introduction

Chromium is one of the most important heavy metal in the environment. It is mainly present in two oxidation states, Cr(III) and Cr(VI), depending on the redox conditions. Cr(VI) is the carcinogenic form of chromium, while trace amount of Cr(III) is essential for healthy growth (Lv *et al*., 2014). Acute exposure to Cr(VI) causes nausea, diarrhea, liver and kidney damage, dermatitis, internal hemorrhage, and respiratory problems. Inhalation may cause acute toxicity, irritation and ulceration of the nasal septum and respiratory sensitization (asthma) (Mohan *et al*., 2006).

Several treatment technologies have been developed to remove chromium from water and wastewater. Common methods include chemical precipitation, ion exchange, membrane separation, ultrafiltration, flotation, electrocoagulation, solvent extraction, sedimentation, precipitation, electrochemical precipitation, soil flushing/washing, electrokinetic extraction, phytoremediation, reduction, reverse osmosis, dialysis/electrodialysis, adsorption/filtration, evaporation, cementation, dilution, air stripping, steam stripping, flocculation, and chelation (Roundhill and Koch, 2002). Chromium removal using several type of natural or commercial zeolites have been studied in the past (Covarrubias *et al*., 2006).

The aim of this work is the removal of hexavalent chromium from aqueous solutions using new adsorbent materials based on activated carbon, modified zeolites with HDTMA – Br and goethite. Adsorption kinetics such as pseudo – first order, pseudo – second order, Elovich and Intraparticle diffusion models were applied to the experimental data.

2. Materials & methods

2.1. Production of adsorbents

Goethite was prepared according to Schwertmann and Cornell method (1991) having a specific surface area equal to 32.0 $m^2 g^{-1}$. Clinoptilolite was bought from S&B Company (Greece). It has a cation exchange capacity equal to 2.35 meq g^{-1}, specific surface area around 31.0 $m^2 g^{-1}$ and average particle size less than 2 mm. Commercial activated carbon was derived from Merck company. The modification of zeolite (clinoptilolite) with hexadecyltrimethylammonium-bromide (HDTMA-Br) was described elsewhere (Brozou *et al*., 2013).

G-MZ I was prepared by adding 20 g of modified zeolite with HDTMA – Br, 50 mL $Fe(NO_3)_3$ 1M and 80 mL KOH 5M to 1 L of polyethylene flask. The suspension was diluted to 1 L with twice distilled water and was held in a closed polyethylene flask at 70ºC for 300 h. Then, the flask was removed from the oven and the precipitate was filtered, washed with twice distilled water and finally dried for 3 days. The same procedure was followed for G-MZ-C I but instead of adding 20 g of modified zeolite with HDTMA – Br in the beginning of the experiment, we add 10 g of modified zeolite with HDTMA – Br and 10 g of commercial activated carbon.

G-MZ II was prepared by adding 50 mL $Fe(NO_3)_3$ 1M and 80 mL KOH 5M to 1 L of polyethylene flask. The suspension was diluted to 1 L with twice distilled water and was held in a closed polyethylene flask at 70ºC for 92 h. Then, the flask was removed from the oven and 20 g of modified zeolite with HDTMA – Br were added. The flask remained to the oven at 70ºC for 100 h and then the precipitate was filtered, washed with twice distilled water and finally dried for 2 days. The same procedure was followed for G-MZ-C II but instead of adding 20 g of modified zeolite with HDTMA – Br in the end of the experiment, we add 10 g of modified zeolite with HDTMA – Br and 10 g of commercial activated carbon.

2.2. Characterization of adsorbents

The infrared spectra (FTIR) of the adsorbents were obtained using a Perkin Elmer spectrophotometer. All FTIR images were taken and collected in transmission mode in the region of 4000-500 cm^{-1} at a resolution of 4 cm^{-1}.

2.3. Preparation of Cr(VI) solution

Aqueous solution of hexavalent chromium was prepared from $K_2Cr_2O_7$, in a concentration of 40 ppm. An amount of each adsorbent was placed in plastic tubes in a proportion of adsorbent to adsorbate equal to 1/100 g mL^{-1}. The samples were equilibrated, centrifuged at 12000 rpm for 5 min and then filtration was followed. Cr(IV) was determined with di – phenyl – carbazide method using a Shimadzu UV-VIS spectrophotometer at 540 nm (American Public Health Association *et al*., 1999). The adsorbed amount (q_t) of Cr(VI) onto the adsorbent was determined from the difference between the initial amount of adsorbate (q_o) in the solution and the corresponding measured amount of the adsorbate in every sample of solution expressed as %, i.e. q_t $100/q_o$ or mg Cr(VI) / g adsorbent.

2.4. Kinetic analysis

Different kinetic models were used to investigate the mechanism of adsorption (Ioannou and Simitzis, 2009).

The pseudo-first-order kinetic model is given by the following equation:

$$\log(q_e - q_t) = \log q_e - \frac{k_1}{2.303} t \quad (1)$$

where q_e and q_t are the amounts, mg, of dye adsorbed per unit mass of adsorbent at equilibrium and at time t, respectively and k_1 is the equilibrium rate constant of pseudo-first-order adsorption ($mgg^{-1}min^{-1}$). The slope of the plot of $\log(q_e - q_t)$ versus t was used to determine k_1 (mgg^{-1} min^{-1}) and the intercept q_e.
The pseudo – second order kinetic model can be expressed as follows:

$$\frac{t}{q_t} = \frac{1}{k_2 q_e^{\,2}} + \frac{t}{q_e} \tag{2}$$

where k_2 (mgg^{-1} min^{-1}) is the equilibrium rate constant of pseudo-second-order adsorption. The slope of the plot of t/q_t versus t was used to determine q_e and then from the intercept, k_2 was calculated.

Elovich equation is expressed as follows:

$$q_t = \frac{1}{\beta}\ln(\alpha\beta) + \frac{1}{\beta}\ln t \tag{3}$$

where α ($mgg^{-1}min^{-1}$) is the initial sorption rate, and the parameter β (mgg^{-1}) is related to the extent of surface coverage and activation energy for chemisorption. If this equation is valid, then a straight line is arisen by plotting q_t versus lnt. The slope of the plot was used to determine $1/\beta$, and then from the intercept, $\ln(\alpha\beta)/\beta$ is calculated.
Adsorption kinetics is usually controlled by different mechanisms such as diffusion. The intraparticle diffusion model can be defined as:

$$q_t = k_{id} t^{0.5} + C \tag{4}$$

where q_t is the amount adsorbed at time t, C is a constant and k_{id} ($mgg^{-1}min^{-0.5}$) is the intraparticle diffusion rate constant. If the regression of q_t versus $t^{0.5}$ is linear and passes through the origin, then intraparticle diffusion is the sole rate-limiting step.

The applicability of the data from kinetic analysis and isotherms were further validated by the normalized standard deviation, Δq (%), which is defined as (Cazetta *et al*., 2011):

$$\Delta q(\%) = 100\sqrt{\frac{\sum[(q_{t,\exp} - q_{t,theor.})/q_{t,\exp}]^2}{N-1}} \tag{5}$$

where N is the number of data points, $q_{t,exp}$ and $q_{t,theor.}$ (mgg^{-1}) are the experimental and calculated adsorption uptake, respectively. The higher is the value of r^2 and the lower is the value of Δq (%) the better will be the goodness of fit.

3. Results & discussion

According to the FTIR analysis (Fig.1), the spectra of G-MZ I and G-MZ-C I adsorbents differ from the spectra of G-MZ II and G-MZ-C II due to the lack of wavenumbers at 897 and 793 cm^{-1} which correspond to inner surface Al-OH deformation and stretching vibration modes of O-T-O groups (T = Si and Al) or –OH out of plane bending, respectively. The strong peak at 980-1005 cm^{-1} corresponds to Si-O planar stretching or C-N stretching due to the presence of nitrogen in HDTMA-Br. Bending vibrations of T-O bonds (T = Si and Al) and Fe-O symmetric streching are present at 430-450 cm^{-1} and 576-640 cm^{-1}, respectively. Functional groups such as –OH and -C-H are also present at 3100-3370 cm^{-1} and 2920, 2850 cm^{-1}, respectively while CH_3-R asymmetric stretching appeared at 1350-1370 cm^{-1}. The functional groups of commercial activated carbon that exist in tripartite adsorbents were difficult to be identified, due to their low concentration and proportion in comparison to the element of carbon and due to the spectrum background (Covarrubias *et al*., 2006).

The adsorption curves for all materials reach equilibrium after a certain time (Fig.2). It is observed that all adsorbents lead to overall adsorption of Cr(VI) (90 - 100%) except for G-MZ II

which presents almost 78% of Cr(VI) adsorption. All adsorbents reached equilibrium in 120 minutes. The adsorption capacity of the materials increases according to the order: G – MZ II < G – MZ I < G – MZ – C II ≤ G – MZ – C I. According to the amount of Cr(VI) adsorbed per unit mass of adsorbent (Fig. 2b), G – MZ – C I adsorbed the highest amount of Cr(VI) equal to 3.835 mg/g of adsorbent while G – MZ II adsorbed the lowest amount of Cr(VI) equal to 3.135 mg/g of adsorbent. All the other adsorbents presented intermediate Cr(VI) adsorption values.

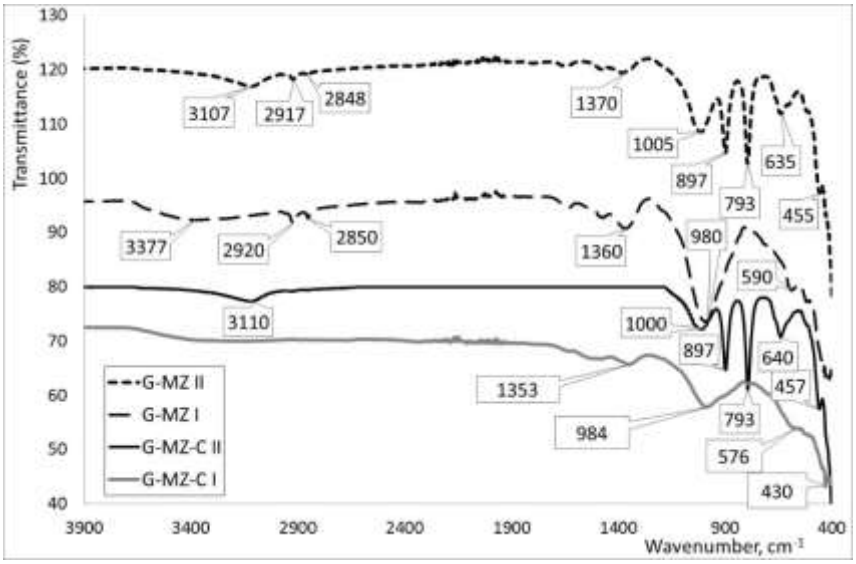

Figure 1: FTIR characterization of the adsorbents

Zeolites are aluminosilicate materials with high surface area and cation exchange capacity (C.E.C.). (Bhatnagar and Minocha, 2006). Cr(VI) adsorption capacity from modified zeolites, increases significantly due to the modification of zeolite surface from negatively to positively charged due to the positively charged head group of the sorbed HDTMA layer. The faster adsorption of Cr(VI) on tripartite systems in comparison with the binary systems, was caused due to the presence of commercial activated carbon, which has a porous structure and a network of interconnected macropores, mesopores and micropores resulting in large surface area and good capacity (Aksu and Yener, 2001).

Chromate ions may exist in aqueous solutions in different ionic forms depending on the pH and the solution concentration. Bichromate ions ($Cr_2O_7^{2-}$) dominate in acidic environments for chromium concentrations higher than 500 mg/L while other forms such as $HCrO_4^-$ and CrO_4^{2-} oxyanions dominate at concentrations below 500 mg/L. Between pH 2 and 6, $HCrO_4^-$ and dichromate ion, $Cr_2O_7^{2-}$ are in equilibrium, while above pH 6, CrO_4^- species predominate. Below pH 1, the Cr(VI) species are presented as $HCr_2O_7^-$ ions (Baes and Mesmer, 1976).

Chromate ions either in univalent or in divalent form displace the surfactant counter ion from the exchange sites on the clays forming Clin-HDTMA-$HCrO_4$, (Clin-HDTMA)$_2$-Cr_2O_7, (Clin-HDTMA)$_2$-CrO_4, Clin-HDTMA-HCr_2O_7, respectively, where Clin-HDTMA- is the modified clinoptilolite with HDTMA-Br exchanging Br^- ions with the different species of chromate ions (Krishna *et al*., 2001). In our experiment, the solution pH ranged from 8 to 9.7, indicating that the prevailing anions in the solution are mainly divalent anions CrO_4^{2-} and were adsorbed by modified zeolites in the form of (Clin-HDTMA)$_2$-CrO_4. In addition, the lower affinity of Cr(VI) sorption at pH 10 may also be influenced by the strong competition from OH^- with Br^- or chromate anion for the sorption sites since more OH^- anions are present at high pH (Yusof and Malek, 2009).

According to Fig.2b, the experimental curves which represent the amount of adsorbate, Cr(VI), adsorbed per unit mass of adsorbent are plotted versus $t^{1/2}$. Four regions can be distinguished (see Table1). From the slope of the straight line, the rate parameter k_{id} is determined (Table 2).

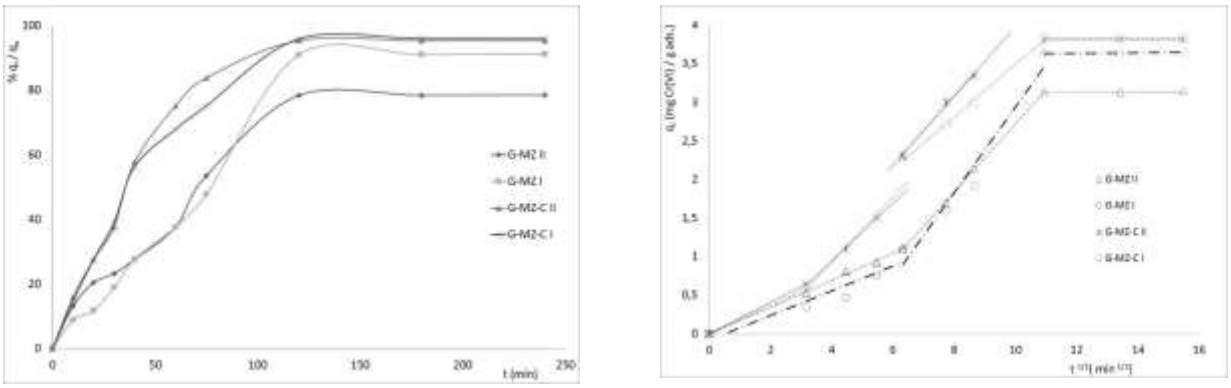

(a) (b)

Figure 2: (a) Adsorption percentage and (b) kinetics of Cr(VI) uptake according to the Intraparticle diffusion model for the proportion of adsorbent-to-solution ratio equal to 10 g of adsorbent L^{-1} of Cr(VI) in solution.

Table 1: The four regions according to Fig.2 for the adsorption of Cr(VI) on adsorbents

Adsorbent	Regions (t in min)			
	A (1st line)	B (2nd line)	C (3rd line)	D (4th line)
G – MZ I	0 – 40	-	40 – 120	120 – 240
G – MZ II	0 – 40	-	40 – 120	120 – 240
G – MZ – C I	0 – 10	10 – 40	40 – 120	120 – 240
G – MZ – C II	0 – 10	10 – 40	40 – 120	120 – 240

According to normalized standard deviation, Δq (%) and correlation coefficient factor (r^2) values applied to all kinetic models (Table 2), adsorption data follow Intraparticle diffusion for the tripartite adsorbents (region B) due to the high r^2 values, near unity, and low Δq values compared to all other models applied to region B (2nd line). By applying the same procedure for the C region (3rd line), it was found out that the r^2 values differ slightly from unity and Δq (%) has values lower than 15% for the binary (G–MZ I, G– MZ II) and lower than 6% for the tripartite (G–MZ –C II, G–MZ–C I) adsorbents. Therefore, the parameter k_{id}, determined from the data of the B and C region is characteristic for the rate of adsorption where Intraparticle diffusion is the rate control mechanism. Furthermore, adsorption experiments at higher temperatures than 293.15 K, i.e. 313.15 and 333.15 K (not presented in the present work) have shown that the adsorption is increased significantly at higher temperatures indicating that the overall adsorption process is controlled by intraparticle diffusion of Cr(VI) (Srihari and Das, 2008).

According to the literature (Allen *et al*., 1989), the initial portion (1st line), A region, represents the external mass transfer and it is followed by two linear sections (B and C) representing the Intraparticle diffusion. The Intraparticle diffusion parameters for the B and C region were determined from the slope of the plots. The rate parameter for the diffusion in the B and C region is attributed to macropore diffusion and mesopore or transitional pore diffusion (Allen *et al*., 1989). Above C region the final equilibrium stage occurs, which represents D region.

The kinetic models, such as pseudo first order, pseudo second order and Elovich equations, which describe the adsorption of the adsorbate molecules on the interior surface of the pores and capillary spaces have been applied to the experimental data (Table 2). The kinetic models were used for the B and C region according to table 1. The phenomena of Intraparticle diffusion and adsorption are not precisely distinct and consequently the experimental data of the B and C region should be used separately. According to normalized standard deviation, Δq (%) and correlation coefficient factor (r^2) values applied to all kinetic models only Elovich equation is acceptable for the C region (3rd line). Beside the criterion of correlation coefficient factor (r^2) which is high enough for the pseudo-second order model in the C region, normalized standard

deviation, Δq (%) is high enough (>100%) indicating the inappropriateness of the model for the C region. All other kinetic models cannot describe the adsorption data since they presented high normalized standard deviation values and low correlation coefficient factor values.

Table 2: Kinetic constants of four models for Cr(VI) adsorption from aqueous solutions on adsorbents

Models	2nd line				3rd line			
Pseudo-First order	k_1(min^{-1})	$^*q_{e,cal}$ (mg·g^{-1})	r^2	Δq (%)	k_1(min^{-1})	$^*q_{e,cal}$ (mg·g^{-1})	r^2	Δq (%)
G – MZ I	-	-	-	-	0.072	110.744	0.866	*H
G – MZ II	-	-	-	-	0.074	89.876	0.897	*H
G – MZ – C I	0.023	4.277	0.963	31.096	0.084	121.101	0.883	*H
G – MZ – C II	0.024	4.263	0.929	29.821	0.104	285.221	0.909	*H
Pseudo-Second order	k_2 (mg·g^{-1}·min^{-1})	$^*q_{e,cal}$ (mg·g^{-1})	r^2	Δq (%)	k_2 (mg·g^{-1}·min^{-1})	$^*q_{e,cal}$ (mg·g^{-1})	r^2	Δq (%)
G – MZ I	-	-	-	-	$5.563\cdot10^{-5}$	21.207	0.369	*H
G – MZ II	-	-	-	-	$2.745\cdot10^{-5}$	32.756	0.495	*H
G – MZ – C I	$5.030\cdot10^{-5}$	33.901	0.191	*H	$2.349\cdot10^{-3}$	6.018	0.987	*H
G – MZ – C II	$3.030\cdot10^{-4}$	14.372	0.247	*H	$3.431\cdot10^{-3}$	5.546	0.991	*H
Intraparticle diffusion	k_{id} (mg·g^{-1}·min$^{-0.5}$)		r^2	Δq (%)	k_{id}(mg·g^{-1}·min$^{-0.5}$)		r^2	Δq (%)
G – MZ I	-		-	-	0.554		0.956	14.269
G – MZ II	-		-	-	0.441		0.999	0.960
G – MZ – C I	0.513		0.970	10.463	0.341		0.998	0.790
G – MZ – C II	0.505		0.998	13.920	0.316		0.944	5.131
Elovich equation	β (mg·g^{-1})	α (mg·g^{-1}·min^{-1})	r^2	Δq (%)	B (mg·g^{-1})	α (mg·g^{-1}·min^{1})	r^2	Δq (%)
G – MZ I	-	-	-	-	0.783	0.075	0.998	18.052
G – MZ II	-	-	-	-	0.537	0.081	0.991	5.219
G – MZ – C I	0.878	0.172	0.930	15.308	0.695	0.164	0.985	2.854
G – MZ – C II	0.900	0.175	0.888	18.587	0.733	0.197	0.978	3.105

*where $q_{e,cal}$ the calculated through models adsorbed amount of Cr(VI) in equilibrium per g of adsorbent, *H the high values of Δq (%), above 100%

4. Conclusions

- FTIR analysis has shown that the appropriate method I or II used for the production of each adsorbent led to different adsorptive materials. The infrared spectra of G-MZ I and G-MZ-C I do not present the peaks at 897 and 793 cm^{-1} which correspond to inner surface Al-OH deformation and stretching vibration modes of O-T-O groups (T = Si and Al) or –OH out of plane bending, respectively as it happens with G-MZ II and G-MZ-C II.
- FTIR analysis has shown the presence of functional groups, i.e. Si-O, C-N, Al-O, –OH, -C-H, CH_3-R and Fe-O.
- The adsorption capacity of adsorbents increases in the following order: G–MZ –C II $\geq$ G–MZ–C I> G– MZ I > G–MZ II
- From the application of the kinetic models, it is concluded that: (a) the intraparticle diffusion model is valid for the B and C region where macropore and mesopore diffusion takes place, respectively and (b) the Elovich kinetic model for the adsorption of Cr(VI) on all adsorbents for the C region
- Tripartite adsorbents consisting of zeolite modified with HDTMA, goethite and activated carbon can be used as filters in operations combining the adsorption properties of carbons and zeolites.

REFERENCES

1. Aksu Z. and Yener J. (2001), A comparative adsorption/biosorption study of mono-chlorinated phenols onto various sorbents, Waste Manage., **21**, 695-702.
2. Allen S. J., McKay G. and Khader K.Y.H. (1989), Intraparticle diffusion of a basic dye during adsorption onto sphagnum peat, Environ.Pollut., **56**, 39-50.
3. American Public Health Association, American Water Works Association, Water Environment Federation (1999), Standard Methods for the examination of water and wastewater. Washington D. C., p.p. 421-426
4. Baes C.F. and Mesmer R.E. (1976), The hydrolysis of cations, John Wiley & Sons, New York.
5. Bhatnagar A. and Minocha A. K. (2006), Conventional and non-conventional adsorbents for removal of pollutants from water-A review, Indian J. Chem. Technol. **13**, 203-217.
6. Brozou E., Ioannou Z., Antoniadis V. and Dimirkou A. (2013), Adsorption of hexavalent chromium from aqueous solutions onto modified zeolites, Proceedings of the 13th International Conference on Environmental Science and Technology, Athens, 5-7 September 2013.
7. Cazetta A. L., Vargas A. M. M., Nogami E. M., Kunitta M. H., Guilherme M. R., Martins A. C., Silva T. L., Moraes J. C. G. and Almeida V. C. (2011), NaOH-activated carbon of high surface area produced from coconut shell: Kinetics and equilibrium studies from the methylene blue adsorption, Chem. Eng. J., **174**, 117-125.
8. Covarrubias C., García R., Arriagada R., Yánez J., Garland T. (2006), Cr(III) exchange on zeolites obtained from kaolin and natural mordenite, Microporous Mesoporous Mater., **88**, 220-231.
9. Ioannou Z. and Simitzis J. (2009), Adsorption kinetics of phenol and 3-nitrophenol from aqueous solutions on conventional and novel carbons, J. Hazard. Mater., **171**, 954-964.
10. Krishna B.S., Murty D.S.R. and Jai Prakash B.S. (2001), Surfactant – modified clay as adsorbent for chromate, Appl. Clay. Sci., **20**, 65-71.
11. Lv G., Li Z., Jiang W.-T., Ackley C., Fenske N., Demarco N., (2014), Removal of Cr(VI) from water using Fe(II)-modified natural zeolite, Chem. Eng. Res. Des., **92,** 384-390.
12. Mohan D., Singh K.P., Singh V.K. (2006), Trivalent chromium removalfrom wastewater using low cost activated carbon derived from agricultural waste material and activated carbon fabric cloth, J. Hazard. Mater., **135,** 280–295.
13. Roundhill D.M. and Koch H.F. (2002), Methods and techniques for the selective extraction and recovery of oxoanions, Chem. Soc. Rev **31**, 60–67.
14. Schwertmann, U. and Cornell R. M. (1991), Iron oxides in the laboratory, Preparation and Characterization, VCH Publications, New York, p.p. 101-110
15. Srihari V. and Das A. (2008), The kinetic and thermodynamic studies of phenol-sorption onto three agro-based carbons, Desalination, **225**, 220-234.
16. Yusof A.M. and Malek N.N. (2009), Removal of Cr(VI) and As(V) from aqueous solutions by HDTMA-modified zeolite Y, J. Hazard. Mater., **162**, 1019–1024.